COBEM 2023 27TH INTERNATIONAL CONGRESS OF MECHANICAL ENGINEERING

ABCM Brazilian Society of Mechanical Sciences and Engineering
27th ABCM International Congress of Mechanical Engineering
December 04-08, 2023, Florianópolis-SC, Brazil

COB-2023-1180
INFLUENCE OF WELDING SPEED ON THE MACRO AND MICROSTRUCTURE OF 316L-SI STAINLESS STEEL OVERLAY WELDS OBTAINED BY GMAW

Anderson Eduardo de Salles Oliveira
Raquel Almeida Calado
Joyce Ingrid Venceslau de Souto
Federal University of Campina Grande, Aprígio Veloso st., 882 - Bloco BL
andersonsalles154@gmail.com, raquel.almeida@estudante.ufcg.edu.br, joyceingrid.cg@gmail.com

Jefferson Segundo de Lima
Federal University of Campina Grande, Aprígio Veloso st., 882 - Bloco BL
jefferson.segundo@ufpe.br

Abstract. *Among GMAW (Gas Metal Arc Welding) applications, overlay welding stands out across various industrial sectors due to its ability to enhance the mechanical and electrochemical properties of surfaces, while making use of more cost-effective substrates. In the context of this coating process, austenitic stainless-steel alloys find extensive use, particularly AISI 316L-Si, renowned for its remarkable corrosion resistance and excellent workability. It's imperative to emphasize that, beyond scrutinizing the process and the choice of steel, the analysis of welding parameters holds even greater significance. These parameters impact not only the weld's geometry, quality, and microstructure but also the formation of the heat-affected zone (HAZ) and the eventual mechanical properties. Hence, this study aims to assess the impact of varying welding speed on the geometric and microstructural characteristics of 316L-Si austenitic stainless steel overlay welds obtained through GMAW. To conduct this experimental analysis, a comprehensive literature review was performed and the weld deposits were proceeded to fabrication. It was altered a single parameter, namely the welding speed, while maintaining the consistency of the remaining parameters, carefully selecting the ones yielding best outcomes as suggested by the literature. Across the various samples, it was delved into the geometric features, the temporal evolution of voltage and current, and the grain size within the weld metal and HAZ regions. Notably, the hardness profile retained a steady state in one of the samples, even in regions with coarser grains, whereas the other sample exhibited a hardness peak within the same region. Furthermore, the sample with the lowest speed, 4.17 mm/s, displayed reduced values for dilution, height, and width in the depositions, even though it had a higher heat input. Conversely, the sample with the highest speed, 5.83 mm/s, exhibited elevated dilution values and a broader HAZ. Key factors like the deposition level and penetration depth played pivotal roles in comprehending these outcomes. Hence, the results highlight how even a minor variation in speed can instigate significant alterations in the characteristics and properties of the final structure. This underscores the critical importance of conducting comprehensive welding experiments, be it in a research or industrial context.*

Keywords: *309LSi coatings, overlay welding, automated GMAW, heat input*

1. INTRODUCTION

One of the primary overlay welding processes utilized in the industry is the Gas Metal Arc Welding (GMAW) process, known as a well-regarded and efficient process that can be semi-automated, user-friendly, and highly productive (BAUMGAERTNER FILHO, 2017). In this welding process, an electric arc is established between the workpiece and a continuously fed bare solid electrode. The resulting molten pool is shielded by an inert or oxidizing (active) gas or a combination of gases (MACHADO, 1996). Fusion welding necessitates the application of heat to melt both the base metal and the filler metal, resulting in a well-structured welded joint with favorable mechanical and metallurgical properties upon solidification. Therefore, heat input is a crucial factor in welding, particularly in determining the geometry of the weld bead. It can be measured by considering welding parameters such as welding current and voltage, plus the speed at which the torch is displaced (Madavi; Jogi; Lohar, 2022).

Heat input is the amount of heat deposited in a material and it plays a crucial role in shaping the microstructure of a welded joint. During the welding process, the base and filler metals are heated to high temperatures and then cooled rapidly, resulting in significant changes to the material's microstructure. In this context, it directly affects the cooling rate of the welded joint. While a slow cooling allows the material to undergo specific microstructural transformations, a lower heat input results in faster cooling, which can lead to a different microstructure.

Welding serves various purposes, and one notable application is metal overlaying. This process involves depositing a layer of filler metal onto the surface of another metal, with the aim of achieving specific properties or dimensions (PHILLIPS, 1965b). In this context, according to Baumgaertner Filho (2017), this welding application has been a trend in the industrial sector as it offers a means of obtaining surfaces with enhanced anti-corrosion and anti-wear properties. The selection of carbon steel as the substrate for stainless steel coating is ideal for applications necessitating both robust mechanical strength and excellent corrosion resistance. This is particularly relevant in industries such as petroleum, petrochemical, shipbuilding, and pressure vessel manufacturing (Di Schino; Testani, 2020). In this context, scientific studies that seek to investigate the effects behind these welding applications are relevant to enhance comprehension and optimize the physical and metallurgical characteristics of coatings for industrial use.

The extensive range of applications for overlays produced through welding, primarily employing stainless steel alloys as filler material, has spurred increased research into the impact of process parameters on microstructure and the enhancement of mechanical properties in coated products (Silva *et al*., 2019). Austenitic stainless steels with low carbon content and the addition of austenite-stabilizing elements, such as 316LSi, are among the most extensively researched in the series. They are known for their excellent corrosion resistance, good ductility, high strength given the presence of elements like Mo, Ni, and Cr (Vora *et al*., 2022; Isquierdo *et al*., 2022). Additionally, these steels exhibit good weldability at elevated temperatures. As an example, Puchi-Cabrera et al. (2007) investigated the impact of metal transfer mode and the O2 content in the shielding gas mixture within the GMAW process on the fatigue life of welded joints in AISI 316L stainless steel. Their analysis focused on how welding process variables could affect the fatigue life of welded joints, a critical factor for ensuring the integrity and longevity of structures constructed using this stainless steel.

It is well-established that coating processes, particularly those with heat input like overlay welding, necessitate specific product characteristics to validate the procedure. These include minimal dilution and penetration values, as well as ideal ratios of reinforcement and deposit width. In this context, comprehending how various input variables of the process effects deposit characteristics is of paramount significance. Consequently, this study aims to explore the effects of welding speed on the macrostructure and metallurgical properties of 316LSi overlay welds obtained through a semi-automated GMAW process. To achieve this, the overlay welds were characterized in terms of macrograph and micrograph to analyze important aspects such as dilution, microstructural and hardness changes with varying welding speed.

2. MATERIALS AND METHODS

2.1 Materials

In the present work, an AISI 1015 steel was used as the base metal and the ER316LSi tubular wire was used as the filler metal. The dimensions of each substrate to be overlayed were 200 mm long x 100 mm wide by 5 mm of thickness. Both nominal chemical compositions are presented in Table 1.

Table 1. Nominal chemical composition (% by weight) of base and filler metal.

Material	C	Ni	Cr	Mn	Si	Mo	Cu	P	S	Fe
Steel AISI 1015	0.148	-	0.043	0.419	-	-	-	-	-	Bal.
Steel ABNT 316L-Si	0.030	12.5	19.0	1.75	0.83	2.5	0.75	0.03	0.03	Bal.

In this scenario, the conventional GMAW was chosen, employing the DigiPLUS A7 welding power supply from IMC Soldagem, for which the built-in equipment was utilized to collect voltage and current data. It is important to highlight that the reference voltage was set at 22.5 V during the weld depositions, while the current fluctuated during the process. Figure 1 illustrates the welding power supply that was employed. The system responsible to perform the overlay weld are constituted of a gas cilinder, the Tartílope V1 model of torch displacement system from IMC Soldagem, the STA-20 wire feeder from IMC Soldagem, and the SAP V4 data acquisition system from IMC Soldagem, that stored the current and voltage data at 5 kHz of rate.

Figure 1. Welding power supply.

The following welding parameters were employed: a voltage (V) of 22.5 V, a wire feed speed of 6 m/min, and the use of commercial pure argon gas (99.98% Ar) as the shielding gas with a flow rate of 16 L/min. Additionally, a consistent distance of 20 mm was maintained from the nozzle to the workpiece at a 90° angle. It is essential to highlight that these parameters were determined through an extensive literature review, drawing from studies such as Ghosh *et al*. (2017), Moslemi *et al*. (2015), and Zumelzu *et al*. (1999), which examined the impact of welding parameters on both micro and macrostructural characteristics of the welded components. The selection process followed a systematic data collection approach, which led to the choice of parameters that demonstrated the most favorable outcomes in previous research. Lastly, the last parameter to consider is welding speed (WS), which was adjusted according to Table 2.

Table 2. Input parameters and its experimental limit.

Experiment	WS, mm/s
1	4.17
2	5.83

The voltage and the welding speed are independent variables when calculating the heat input of the welding, being estimated from Equation 2 (Modenesi, Marques, Santos, 2012):

$$H_l = \eta \cdot \frac{V \cdot I}{WS} \tag{1}$$

Where H_l is the heat input (J/mm); V is the applied voltage (V); I is the electric current (A); WS is the welding speed (mm/s); and η is the thermal efficiency of the process (%).

2.2 Metallographic characterization

According to SANTOS *et al*. (2019) and Zamin (2010), samples should be taken from the cross-section of each sheet in order to obtain the average values and their consequent dilution variations (D). In order to carry out the microstructural analysis, the samples were prepared in the following sequence: hot embedding in resin (bakelite); sanded to 2400 granulometry; polishing in silica solution; chemical etched using Nital 2% for approximately 60 s. For the metallographic analysis, the SC30 model of optical microscopy from Olympus was used to obtain the optical microscopy (OM) images, which were taken of the following areas of the weld metal (WM), heat-affected zone (HAZ) and base metal (BM).

To conduct the macrograph analysis of the weld overlays, the post-processing of the images was performed using Image J software to assess the areas of weld metal reinforcement and base metal penetration in each welded bead to determine the dilution. The dilution (D) is defined as the proportion with which the base metal participates in the molten zone (Modenesi; Marques; Santos, 2012), calculated from Equation 2.

$$D = \frac{A_f}{A_f + A_d} \tag{2}$$

This parameter can be obtained by measuring the areas proportional to the quantities of base metal (A_f) and filler metal (A_d) in a macrograph of the weld cross-section. These output parameters measured by the macrograph are shown in Figure 2.

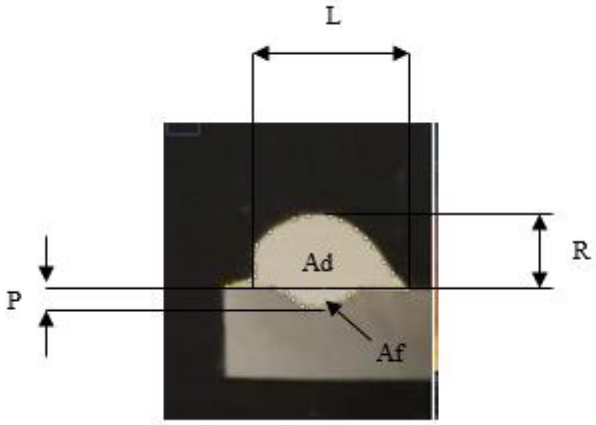

Figure 2. Schematic diagram of output geometric parameters for the overlay welds.

As shown in Figure 2, the height (R), width (L) and penetration (P) of the welds were determined, together with the dilution (D) of the weld metal in relation to the substrate. These mentioned output parameters were used to evaluate the relationship among these and the welding speed, as well as the heat input.

2.3 Hardness test

For the Vickers hardness test, carried out in the Future-Tech model of digital microdurometer from FM-700, a load of 100 g was used for an indentation time of 15 s. Eight indentations along the entire sample, spaced 0.5 mm apart from each other. Figure 3 illustrates the diagrammatic scheme of the indentations made during the hardness test.

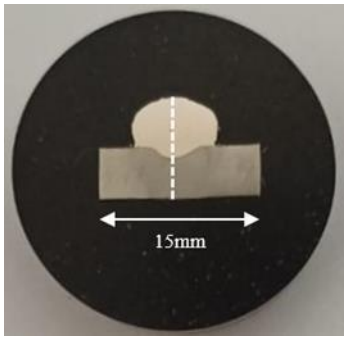

Figure 3. Schematic diagram of the microhardness test indentations.

3. RESULTS AND DISCUSSIONS

3.1 Data Acquisition

In order to calculate the heat input for each weld bead performed, following the experimental methodology described above, it was necessary to collect welding parameters data during the execution of each experiment. Specifically, with both the average welding voltage and current values taken for each bead and considering the thermal efficiency of the GMAW process (Modenesi, P., Marques, P., Santos, 2012), it was possible to calculate the heat input for samples 1 and 2, which are presented in Table 3 for each WS level employed.

Table 3. Experiments with the levels of heat input.

	WS (mm/s)	**V (V)**	**I (A)**	H_l **(J/mm)**
Sample 1	4.17	22.5	152.33	698.62
Sample 2	5.83	22.5	138.51	454.38

By analyzing the heat input results in Table 3, it can be seen that the lowest value of heat input was the result of low values of welding current combined with high values of welding speed, as observed by Krishna Kumar *et al.* (2020), when investigating the effects of different laser welding process parameters on the dissimilar butt welding of nickel 201 and AISI 316 stainless steel. Similar observations were made by Sen *et al.* (2018), when monitoring the influence of

different parameter combinations in the double-pulsed gas metal arc welding (DP-GMAW) process on the microstructural constituents and hardness of low carbon steel weld deposits.

3.2 Macrography

The Figure 4 shows the cross-sectional views of the deposited beads for different levels of WS. Preliminarily, it is already possible to observe notable differences in the parameters L, R, P, and D of the deposits, which were categorically evaluated through post-processing of the macrographs.

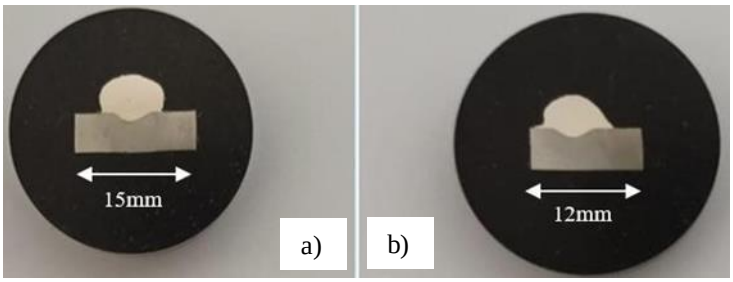

Figure 4. Macrographs of the specimens taken from a) sample 1 and b) sample 2.

The experiments were conducted with a view to the specified WS levels and the samples were cross-sectioned for the analysis of the geometric output parameters mentioned in Table 4.

Table 4. Results of the geometric output parameters from the macrograph.

	R (mm)	**L (mm)**	**P (mm)**	**D (%)**
Sample 1	5.18	7.81	1.31	13.71
Sample 2	4.00	7.18	1.16	10.38

Regarding the reinforcement (R) results, based on the values observed in Table 4, this response is greater when the welding speed is decreased, since its highest value was found for sample 1 ($R = 5.18\,mm$) when compared to sample 2 ($R = 4.00\,mm$), as observed by Gomes *et al.* (2011), which suggests that higher heat input values tend to result in weld beads with higher reinforcement values. A similar analysis refers to the width (L) values, since its results demonstrates that the increase in the welding speed generally causes a considerable increase in the width of the bead, since its highest value was found for sample 1 ($L = 7.81\,mm$) when compared to sample 2 ($L = 7.18\,mm$), also predicted by Gomes *et al.* (2011), when discussing the optimization of multiple characteristics in the cladding process of carbon steel plates using an austenitic stainless steel cored wire. In addition to this, based on the penetration values (P) from Table 4, the highest level of penetration was obtained by sample 1 ($P = 1.31\,mm$) compared to sample 2 ($P = 1.16\,mm$). It can be inferred that weld deposits with higher heat input and lower welding speed are characterized by greater penetration, as predicted by Nogueira (2015), Sánchez-Cruz *et al*. (2023) and Maquiné *et al.* (2019).

Furthermore, for dilution, the results obtained in Table 4 indicates that low percentages of dilution are obtained when simultaneously employing low welding current values with high welding speeds, in agreement with the studies by Carla Silva *et al.* (2019) and Gomes *et al.* (2011). Concerning the efficacy of overlay welds, it is not advisable to exceed dilution values of 20% for a satisfactory overlay in terms of preserving the weld metal characteristics (Nunes *et al.*, 2015). Generally, low dilution levels were observed, with sample 1 recording a dilution of 13.71% and sample 2 recording a dilution of 10.38%.

3.3 Characterization of overlay welds

The metallographic analysis showed the weld metal (WM) together with the zones present in the HAZ, which are: coarse-grained zone (CGHAZ), fine-grained zone (FGHAZ), inter-critical zone (ICHAZ) and the sub-critical region, which is the base metal (BM), as well as the fusion line (FL). From this, the microstructures obtained from samples 1 and 2 are observed in Figures 5 and 6, with heat inputs equivalent to 698.62 J/mm and 454.38 J/mm, respectively.

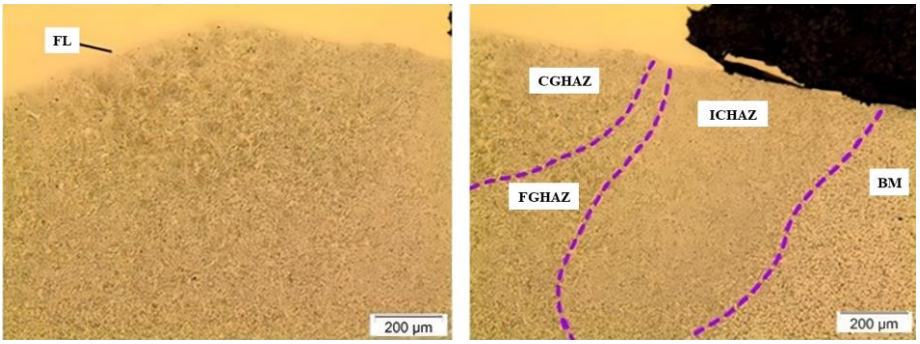

Figure 5. Micrograph of sample 1. Etch: nital 2%.

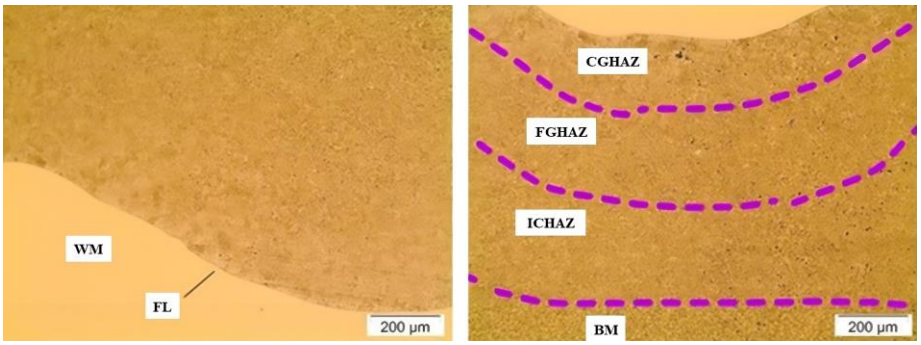

Figure 6. Micrograph of sample 2. Etch: nital 2%.

It can be seen that more extensive HAZ were obtained in the experiment with the lowest welding speed, i.e. sample 1. This phenomenon can be explained by Equation 1. From this mathematical model, it can be seen that the heat input is inversely proportional to the welding speed, so the lower the welding speed, the higher the heat input. Therefore, just as Nunes *et al*. (2012) and Chacón-Fernández *et al*. (2022) concluded, the experiment with the lowest welding speed (sample 1) showed a more extensive HAZ with a coarser grain size than the one with the highest speed (sample 2), preliminarily visualized in the images on the left of Figures 5 and 6.

3.4 Hardness results

Figure 7 shows the hardness profile obtained from the samples 1 and 2, along the regions of WM, HAZ, and BM. Considering that the indentation point count starts in the base metal and increases toward the weld metal, for sample 1, with a welding energy of 698.62 J/mm, it was found that the WM exhibited a lower hardness level compared to sample 2, with a welding energy of 454.38 J/mm. No significant differences in hardness values were observed for the HAZ and BM.

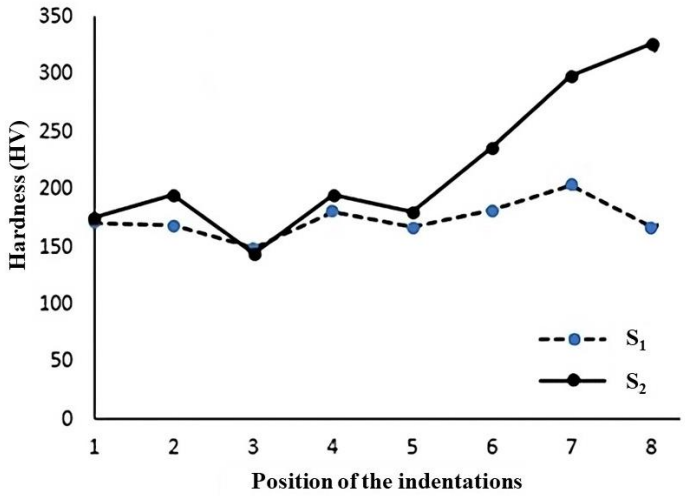

Figure 7. Vickers hardness profiles along the welded joints.

This can be explained by the aspects discussed on previous sections, regarding heat input levels and the relationship between welding speed and cooling rate. For the values obtained for the sample 2, as well as Chacón-Fernández *et al*. (2022) observed, their hardness profile demonstrated constant values at the beginning of the HAZ and a hardness peak when approaching the region of the weld metal, due to the high cooling rate in consequence of a lower heat input. The opposite can be stated regarding sample 1. Figures 8 and 9 shows the micrographs with the results obtained.

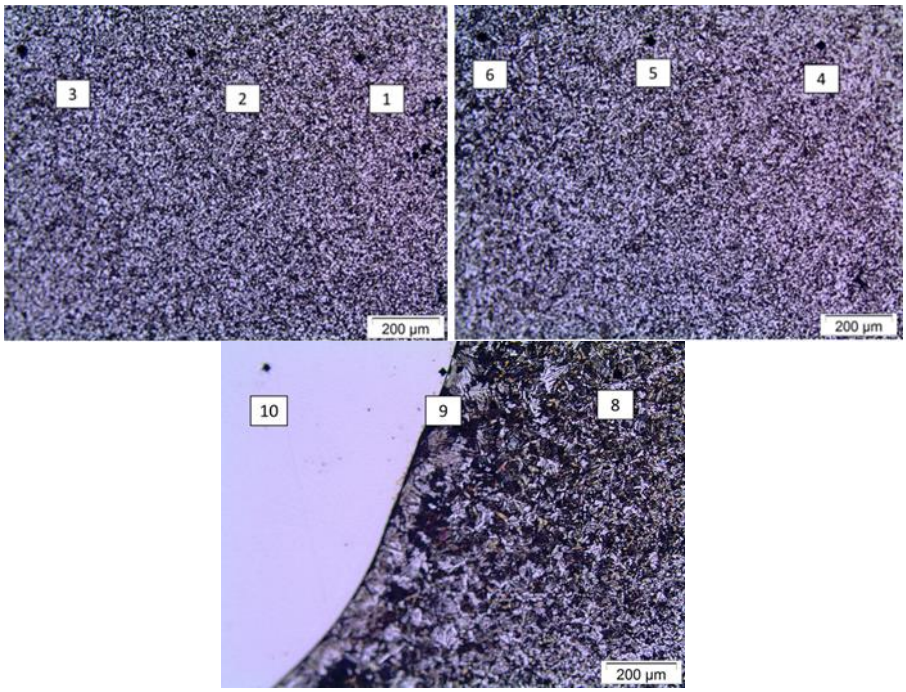

Figure 8. Micrograph of indentations from sample 1.

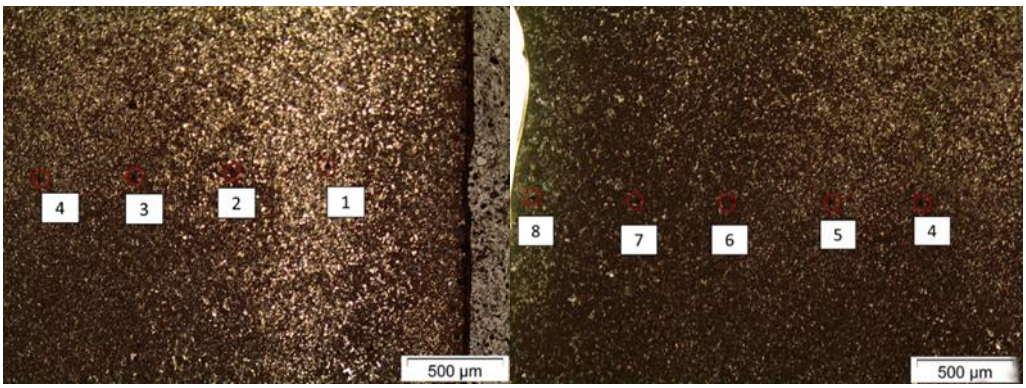

Figure 9. Micrograph of indentations from sample 2.

4. CONCLUSIONS

With the aim of investigating the metallurgical effects on a single weld bead for potential overlay applications, an experimental analysis was conducted using the semi-automated GMAW process. The methodology and process parameters were established based on a thorough literature review. Following this, the weld deposit was obtained and two samples were subsequently extracted for analysis.

Regarding to the geometric characteristics, the welding speed had direct influence on the parameters of heat input, reinforcement, width, penetration and dilution of the weld bead. Lower level of welding speed generated higher heat input and as a result, higher values of reinforcement and width, as well as penetration and dilution, were observed in the analyzed samples. Overall, good results for dilution were obtained at both applied welding speed levels (13.71% for sample 1, and 10.38% for sample 3), considering the recommendations provided by the literature for overlay welds.

In the metallographic analysis, it was observed distinct microstructures in samples 1 and 2. Sample 1, deposited with a lower welding speed, had a higher heat input, resulting in a broader HAZ (heat-affected zone). In contrast, sample 2, obtained with a higher welding speed, had a lower heat input, leading to a thinner HAZ (heat-affected zone) and a more fine-grained microstructure overall due to the faster cooling rate. Although sample 1 had higher welding energy, both

samples had a constant voltage value. As a result, sample 1 had greater deposition, leading to reduced penetration into the base metal.

In the microhardness analysis, while the base metal and the heat-affected zone did not show significant changes in the samples, it is evident that the welding speed affected the hardness of the weld metal, directly related to the cooling rate of the deposit. Sample 2, deposited with a lower level of heat input, obtained higher hardness levels on the weld metal due to the high level of welding speed and, because of that, a greater cooling rate. Therefore, it can be concluded that this work successfully achieved its objective, given that it was possible to observe series of implications on 316LSi overlay weld GMAW-based caused by varying process parameters, such as the welding speed.

5. ACKNOWLEDGEMENTS

The authors would like to express their profound gratitude to the Federal University of Campina Grande (UFCG), the Department of Mechanical Engineering (DEM) from UFCG, and the Welding Laboratory (LabSol) from UFCG for their invaluable technical and human resources, which were instrumental in enabling the completion of this work.

6. REFERENCES

Chacón-Fernández, S., Portolés García, A., & Romaní Labanda, G. (2022). Influence of parameters on the microstructure of a duplex stainless steel joint welded by a GMAW welding process. *Progress in Natural Science: Communication of State Key Laboratories of China*, *32*(4), 415–423. https://doi.org/10.1016/j.pnsc.2022.06.003

Carla Silva, Ana S et al. Aplicação da Metodologia para Qualificação de Procedimentos de Soldagem de Tubulações Industriais Conforme Parâmetros dos Códigos ASME B31.3 e ASME SECTION IX*. Soldagem & Inspeção, [s. l.], p. 14, 2019. Disponível em: https://doi.org/10.1590/0104-9224/SI24.23. Acesso em: 18 dez. 2022.

Di Schino, Andrea; Testani, Claudio. Corrosion behavior and mechanical properties of AISI 316 stainless steel clad Q235 plate. Metals, [s. l.], v. 10, n. 4, p. 1–14, 2020.

Filho, A. J. B. (2017). *Study of Negative Polarity Parameters in MIG/MAG Variable Polarity Welding for Cladding.* 1 Universidade Federal do Rio Grande do Sul – UFRGS.

Fonseca, C. S., Pinheiro, I. P., & Silva, S. N. da. (2016). Influência do aporte térmico sobre a morfologia da austenita e na quantidade das fases em chapas soldadas de aço inoxidável duplex SAF2205. *Matéria (Rio de Janeiro)*, *21*(1), 227–234. https://doi.org/10.1590/s1517-707620160001.0020

Ghosh, N., Pal, P. K., & Nandi, G. (2017). GMAW dissimilar welding of AISI 409 ferritic stainless steel to AISI 316L austenitic stainless steel by using AISI 308 filler wire. *Engineering Science and Technology an International Journal*, *20*(4), 1334–1341. https://doi.org/10.1016/j.jestch.2017.08.002

Gnanasundaram, B. R., & Natarajan, M. (2014). Influences of the heat input on a 2205 duplex stainless steel weld". *Materials and Technology*, 761–763.

Gomes, José Henrique de Freitas et al. Otimização de múltiplos objetivos na soldagem de revestimento de chapas de Aço carbono ABNT 1020 utilizando arame tubular inoxidável austenítico. Soldagem e Inspecao, [s. l.], v. 16, n. 3, p. 232–242, 2011.

Krishna Kumar, G et al. Effect of laser welding process parameters on dissimilar joints of AISI 316 and nickel 201. Materials Today: Proceedings, [s. l.], v. 22, p. 2964–2973, 2020. Disponível em: https://www.sciencedirect.com/science/article/pii/S2214785320322112.

Isquierdo, D. V., Siqueira, R. H. M., Carvalho, S. M., & Lima, M. S. F. (2022). Effect of the initial substrate temperature on heat transfer and related phenomena in austenitic stainless steel parts fabricated by additive manufacturing using direct energy deposition. *Journal of Materials Research and Technology*, *18*, 5267–5279. https://doi.org/10.1016/j.jmrt.2022.04.143

Machado, I. G., Modenesi, P. J., Marques, P. V., & Santos, D. B. (1996). *Soldagem & técnicas conexas: processos. Porto Alegre. editado pelo autor*. UFMG.

Madavi, K R; Jogi, B F; Lohar, G S. Investigational study and microstructural comparison of MIG welding process for with and without activated flux. Materials Today: Proceedings, [s. l.], v. 51, p. 212–216, 2022. Disponível em: https://www.sciencedirect.com/science/article/pii/S2214785321038311.

Maquiné, M. (2022). Influência da variação dos parâmetros do processo de soldagem MIG (GMAW) no comportamento das propriedades mecânicas de juntas soldadas em aço naval ASTM 131 grau A. *Revista de Educação, Ciência e Tecnologia Do IFAM*.

Modenesi, P., Marques, P., Santos, D. Introdução à metalurgia da soldagem. 1. ed. [S. l.: s. n.], 2012. Disponível em: http://demet.eng.ufmg.br/wp-content/uploads/2012/10/metalurgia.pdf.

Moslemi, N., Redzuan, N., Ahmad, N., & Hor, T. N. (2015). Effect of current on characteristic for 316 stainless steel welded joint including microstructure and mechanical properties. *Procedia CIRP*, *26*, 560–564. https://doi.org/10.1016/j.procir.2015.01.010

Nogueira, R. M. U. (2015). *Weld bead variability in mig/mag and flux-cored wire welding processes. Thesis (PhD) - Postgraduate Program in Mechanical Engineering*.

Nunes, Everton Barbosa et al. Avaliação do Efeito da Energia de Soldagem na Deposição de Aço Inoxidável Superduplex pelo Processo Plasma Pó. Soldagem & Inspeção, [s. l.], v. 20, n. 2, p. 205–218, 2015.

Nunes, E. (1965). Influence of Welding Energy on the Microstructure and Microhardness of Duplex Stainless Steel Coatings. Universidade FederaI do Ceará, Ceará. *June*, *3*.

Puchi-Cabrera, E. S., Saya-Gamboa, R. A., La Barbera-Sosa, J. G., Staia, M. H., Ignoto-Cardinale, V., Berríos-Ortiz, J. A., & Mesmacque, G. (2007). Fatigue life of AISI 316L stainless steel welded joints, obtained by GMAW. *Revista de Metalurgia*, *43*(3). https://doi.org/10.3989/revmetalm.2007.v43.i3.67

Ragu Nathan, S., Balasubramanian, V., Malarvizhi, S., & Rao, A. G. (2015). Effect of welding processes on mechanical and microstructural characteristics of high strength low alloy naval grade steel joints. *Defence Technology*, *11*(3), 308–317. https://doi.org/10.1016/j.dt.2015.06.001

Roldão, A. M. B. (2010). *Study of the effect of thermal input on the mechanical and microstructural properties of Duplex Stainless Steel UNS S 31803 in thick plate, welded by the GMAW process*.

Sánchez-Cruz, T. del N. J., Curiel-López, F. F., López-Morelos, V. H., González-Sánchez, J. A., Ruiz, A., & Carrillo, E. (2023). Optimization of macro and microstructural characteristics of 316L/2205 dissimilar welds obtained by the GMAW-pulsed process. *Materials Today. Communications*, *34*(105401), 105401. https://doi.org/10.1016/j.mtcomm.2023.105401

Santos, A. X. dos, Maciel, T. M., Costa, J. D., Sousa, M. B. de, Prasad, S., Campos, A. R. N., & Santana, R. A. C. de. (2019). Study on influence of the PTA-P welding process parameters on corrosion behavior of Inconel 625 coatings. *Matéria (Rio de Janeiro)*, *24*(1). https://doi.org/10.1590/s1517-707620190001.0619.

Sen, Mainak et al. Effect of double-pulsed gas metal arc welding (DP-GMAW) process variables on microstructural constituents and hardness of low carbon steel weld deposits. Journal of Manufacturing Processes, [s. l.], v. 31, p. 424–439, 2018. Disponível em: http://dx.doi.org/10.1016/j.jmapro.2017.12.003.

Silva, Marcos Mesquita da et al. Caracterização de Solda de Revestimento de AWS 317L Depositados por GMAW Duplo Arame em Aços ASTM A 516 Gr 60 para Uso na Indústria do Petróleo. Revista Eletrônica de Materiais e Processos, [s. l.], v. 15, n. 3, p. 225–233, 2019.

Vora, J., Parikh, N., Chaudhari, R., Patel, V. K., Paramar, H., Pimenov, D. Y., & Giasin, K. (2022). Optimization of bead morphology for GMAW-based wire-arc additive manufacturing of 2.25 Cr-1.0 mo steel using metal-cored wires. *Applied Sciences (Basel, Switzerland)*, *12*(10), 5060. https://doi.org/10.3390/app12105060

Zamin, P. (2010). STUDY OF THE THERMAL CYCLE IN THE HEAT AFFECTED ZONE PRODUCED BY THE MAG WELDING PROCESS. *Lume UFRGS*.

Zumelzu, E., Sepúlveda, J., & Ibarra, M. (1999). Influence of microstructure on the mechanical behaviour of welded 316 L SS joints. *Journal of Materials Processing Technology*, *94*(1), 36–40. https://doi.org/10.1016/s0924-0136(98)00450-6.

7. RESPONSIBILITY NOTICE

The authors are the only responsible for the printed material included in this paper.